

# Carbon-13 Chemical Shift Tensors in Polycyclic Aromatic Compounds. 7.<sup>1</sup> Symmetry Augmented Chemical Shift–Chemical Shift Correlation Spectroscopy and Single Crystal Study of Triphenylene

Robbie J. Iulucci, Cu G. Phung, Julio C. Facelli,<sup>†</sup> and David M. Grant<sup>\*‡</sup>

Contribution from the Department of Chemistry and Center for High Performance Computing, University of Utah, Salt Lake City, Utah 84112

Received July 21, 1997

**Abstract:** A modification is made to the chemical shift–chemical shift, CS-CS, correlation spectroscopy method for measuring shift tensors. This new approach incorporates, in an iterative fashion, the redundancy of information available in the spectrum from congruent nuclei in the unit cell. The redundancy reduces the number of 2D spectra required to determine the full chemical shift tensor. The iterative procedure requires reasonably good starting shift values that may be derived from quantum chemical calculation of nuclear shielding parameters. These theoretical tensor estimates provide approximate spectral patterns used in assigning the experimental peaks. With this technique the 18 unique <sup>13</sup>C tensors in a triphenylene unit cell, which describe 72 spectral peaks, were measured with a precision of 0.52 ppm in the tensor components with use of only three 2D spectra instead of the six normally used in the CS-CS method. The chemical shift tensor analysis indicates that, to relieve intramolecular strain, the molecule deforms from planarity, and the molecular symmetry is left with only a single vertical plane. Shift tensors also reflect the major Kekule structures of triphenylene. Further, chemical shift modeling as a function of molecular geometry was used to probe variations between neutron and X-ray diffraction data.

## Introduction

The symmetrical part of the chemical shift tensor, with its six independent parameters, spatially describes the electronic environment of a nucleus. The chemical shift anisotropies of <sup>13</sup>C nuclei are large and for aromatic nuclei are typically more than 200 ppm. With use of single-crystal NMR experiments these six aromatic tensor parameters can be measured with a precision better than 0.5 ppm. Through chemical shielding calculations, the chemical shift may be interpreted in terms of molecular structure. Thus, chemical shift tensors offer a way to quantify intermolecular interactions in the solid state and to provide a 3D topology of molecules that complements diffraction studies.<sup>1–4</sup>

Traditionally, the principal method for acquiring single-crystal chemical shift tensors<sup>5</sup> involved the use of a goniometer probe to obtain arrays of 1D spectra corresponding to the different crystal orientations for the different sample rotations. The limited resolution of this approach, however, precludes its use in studies of single crystals with more than about 15 magnetically nonequivalent nuclei. The 2D chemical shift–chemical

shift, CS-CS, correlation method<sup>6,7</sup> is much more promising for complex molecules. This two-dimensional NMR approach allows considerably larger numbers (70–100) of spectral peaks in a single crystal to be resolved, and all of the magnetic nonequivalent nuclei in the unit cell to be indexed as a function of the crystal orientation. This indexing follows directly from the spatial correlation explicit in the CS-CS measurements. Unfortunately, the CS-CS approach, as with many other 2D NMR methods, is time consuming and modifications are necessary that reduce the required spectrometer time if the technique is to be used broadly. This problem was addressed recently by a modified 2D CS-CS experiment, using chemical shift modulation for crystals containing relatively few nuclei.<sup>8</sup> We now report herein a new symmetry augmented, SA, modification of the 2D CS-CS method that also ameliorates the inherently time consuming procedure of earlier methods.

When considerable crystal symmetry exists in the unit cell, the SA-CS-CS method capitalizes on the redundancy of information found in 2D correlation spectra. Therefore, the number of data sets required are reduced in number from the standard set of six 2D spectra; hence the time savings. The method, however, requires that the crystal symmetry be known and that the congruent sets of nuclei be identified independently to determine the chemical shift anisotropy from their resonance frequencies. To obtain the correct shift values from a reduced number of 2D peaks, a reasonable initial assignment of these

<sup>†</sup> Center for High Performance Computing.

<sup>‡</sup> Department of Chemistry.

(1) Previous paper in this series: Iulucci, R. J.; Phung, C. G.; Facelli, J. C.; Grant, D. M. *J. Am. Chem. Soc.* **1996**, *118*, 4880.

(2) Iulucci, R. J.; Facelli, J. C.; Alderman, D. W.; Grant, D. M. *J. Am. Chem. Soc.* **1995**, *117*, 2336.

(3) Facelli, J. C.; Grant, D. M. *Nature* **1993**, *365*, 325.

(4) Grant, D. M.; Liu, F.; Iulucci, R. J.; Phung, C. G.; Facelli, J. C.; Alderman, D. W. *Acta Crystallogr.* **1995**, *B51*, 540.

(5) Veeman, W. S. Carbon-13 Chemical Shift Anisotropy. *Prog. NMR Spectrosc.* **1984**, *16*, 193.

(6) Carter, C. M.; Alderman, D. W.; Grant, D. M. *J. Magn. Reson.* **1987**, *73*, 114.

(7) Sherwood, M. H.; Alderman, D. W.; Grant, D. M. *J. Magn. Reson.* **1989**, *84*, 466.

(8) Iulucci, R. J.; Grant, D. M. *Solid State NMR* **1996**, *6*, 55.

spectral peaks to specific carbon atoms in the unit cell is required. This process for obtaining the shielding tensors uses quantum chemical calculations to make an initial approximation of the 2D peak patterns which consequently provides an initial principal axes system of the set of congruent nuclei. Fortunately, recent computational advances in *ab initio* calculations of chemical shielding<sup>9,10</sup> are now sufficiently accurate to predict satisfactorily the tensor's principal values and their orientations from which initial spatial assignments can be made for the sets of congruent nuclei in the crystal's unit cell.

Triphenylene was selected to test this modification because of the high symmetry of the four congruent molecules and large number of peaks, 72, in the crystal. The  $P_{212121}$  crystalline symmetry of triphenylene along with the 4-fold congruency of molecules, fortunately, contains sufficient information that it is possible to determine the complete chemical shift tensor from only a pair of 2D CS-CS spectra containing only three distinct crystal orientations relative to the magnetic field. Additional 2D CS-CS spectra, of course, would provide further redundancies to improve the analysis, but by using a symmetry augmented approach the 18 unique tensors of triphenylene may be derived from the 18 sets of four congruent nuclei (hence 72 total peaks) in a reduced amount of time in spite of the unfavorable relaxation factors. Moreover, triphenylene is especially suitable for further exploring aromaticity in fused ring compounds.<sup>11,12</sup> For instance, the Kekule structures of triphenylene predict that the molecule contains minimal  $\pi$ -electron density in the bonds connecting the outer three aromatic rings. The corresponding elongation of these central C—C bonds with their reduction in  $\pi$ -electron density has also been suggested by diffraction studies.<sup>13,14</sup> The diffraction data also indicate considerable deformations from ring planarity for triphenylene in the solid state. The NMR spectrum of solid triphenylene has been studied previously<sup>15</sup> in powder samples, but these powder data provide neither the orientational information that are highly dependent upon the deformations from planarity nor the improved resolution to study subtle changes in the principal shift values. While a single-crystal study of triphenylene provides these data, an unfortunately long proton  $T_1$  for solid triphenylene made this molecule relatively unfavorable for the typical CS-CS 2D approach.

## Experimental Section

**Crystal Preparation.** Triphenylene, obtained from Aldrich, was purified by sublimation and zone refining. The Bridgman method<sup>16</sup> was used to grow a cylindrical single crystal 5 mm in diameter and 50 mm in length. A piece of the crystal was cut and glued to the open end of a 5 mm NMR tube; this cylindrical sample was approximately 8 mm long. A second piece of the single crystal was ground into a spherical shape that filled the bottom 5 mm of a similar NMR tube. In both cases, epoxy glue was used to mount the crystal in a permanent position in the sample tube and to immobilize the tube in the armature of the probe.

**Spectroscopy.** The initial 2D CS-CS spectrum of the cylindrical sample was acquired with operating frequencies for  $^{13}\text{C}$  and  $^1\text{H}$  of 50.307 and 200.06 MHz, respectively, on a Bruker CXP-200 spectrometer. Three additional 2D CS-CS spectra were acquired on the spherical sample by using a Chemagnetics CMX-200 spectrometer console with operating frequencies identical to the Bruker. All spectra were acquired at ambient temperature, and a previous publication describes in detail the instrumentation including the probe, the flipping mechanism, the pulse sequence required for the CS-CS experiment, external referencing, and optimizing crystal misalignment due to mechanical imperfections.<sup>7</sup> A contact time of 5 ms was employed; the evolution period was incremented in 64 steps with 48 transients per increment; and 512 complex data points were recorded in the acquisition dimension. The dwell time for the evolution period differed from the acquisition dimension to provide adequate resolution in an optimum amount of time. An offset, which ranged  $\pm 500$  Hz for the different data sets, was used for the carbon channel to center the carrier frequency in the middle of the spectrum. The 2D mixing time was 30 ms, a period adequate to reorient the sample and to allow mechanical vibrations to decay. The protons were decoupled with a field strength of 83 KHz, and a flip back pulse was used to restore the remaining proton magnetization to the longitudinal axis after the acquisition period. A recycle delay of 300 s provided the maximum signal-to-noise ratio for a constant amount of time.

The original spectrum, obtained from the cylindrical sample, exhibited a better signal-to-noise as a consequence of an increased filling factor. Unfortunately, this method of mounting the crystal at only its base resulted in the crystal shattering after only one 2D spectrum was secured. The remaining data had to be acquired with the spherical sample. The spectral parameters for the second set of spectra acquired on the Chemagnetics CMX-200 were the same as those reported here for the first spectrum. The set of free induction decays was transferred to a VAX 3100 for analysis where 75 Hz Gaussian line broadening was applied. Zero filling before Fourier transformation produced a 2048 by 2048 point spectrum with a 12 by 20 kHz spectral width. Hypercomplex data sets with quadrature detection in both the evolution and acquisition dimensions were processed to produce pure adsorption mode spectra. The highest pixel in each peak of the 2D contour plot was taken as the position of the spectral peak.

By using a Chemagnetics 9.5 mm pencil probe, the CP/MAS spectrum of triphenylene was acquired at ambient temperature on a Chemagnetics spectrometer operating at 400.13 MHz for  $^1\text{H}$  and 100.62 MHz for  $^{13}\text{C}$ . The spinning speed was 3.36 kHz, the  $^1\text{H}$  decoupling field was 45 kHz, and 1800 transients were accumulated.

## SA-CS-CS Procedure and Results

Neumann's principle requires that any physical property of a crystal must possess at least the symmetry of the point group of the crystal.<sup>17,18</sup> Therefore, the individual tensor components of congruent nuclei are not independent and their interdependencies can be determined with group theory considerations. This principle makes it possible to determine the number of independent chemical shielding tensor components for any of the 32 crystal point groups. Congruency between symmetry-related nuclei, with the exception of transitional and inversion symmetry, does not equate to magnetic equivalence, instead, a congruent set of nuclei normally gives more than one spectral peak for an arbitrary crystal orientation. It is this redundancy in the congruent spectral information that permits the complete six-parameter tensors to be determined with measurements at less than six independent crystal orientations. However, to exploit this redundancy, the sets of peaks must be identified along with their symmetry relationships. Hence, *a priori* assignments for a set of spectral peaks to a group of congruent nuclei in the unit cell must first be established to associate

(9) Facelli, J. C. Shielding Tensor Calculations. In *Encyclopedia of NMR*; Grant, D. M., Harris, R. K., Eds.; John Wiley: London 1996; p 4327.

(10) Chestnut, D. B. *Ab Initio Calculations of NMR Chemical Shielding*. In *Annu. Rep. NMR Spectrosc.* **1994**, 29, 71.

(11) Garratt, P. J. *Aromaticity*; John Wiley and Sons: New York, 1986.

(12) Lewis, D.; Peters, D. *Facts and Theories of Aromaticity*; Macmillan Press: London, 1975.

(13) Ferraris, G.; Jones, D. W.; Yerkess, J. Z. *Krist.* **1973**, 138, 113.

(14) Ahmed, F. R.; Trotter, J. *Acta Crystallogr.* **1963**, 16, 503.

(15) Soderquist, A.; Hughes, C. D.; Horton, W. J.; Facelli, J. C.; Grant, D. M. *J. Am. Chem. Soc.* **1992**, 114, 2826.

(16) Sherwood, J. N. In *Purification of Inorganic and Organic Materials; Techniques of Fractional Solidification*; Marcel Dekker: New York, 1969; Chapter 15.

(17) Bhagavantam, S. *Crystal Symmetry and Physical Properties*; Academic Press: New York, 1966.

(18) Buckingham, A. D.; Malm, S. M. *Mol. Phys.* **1971**, 22, 1127.

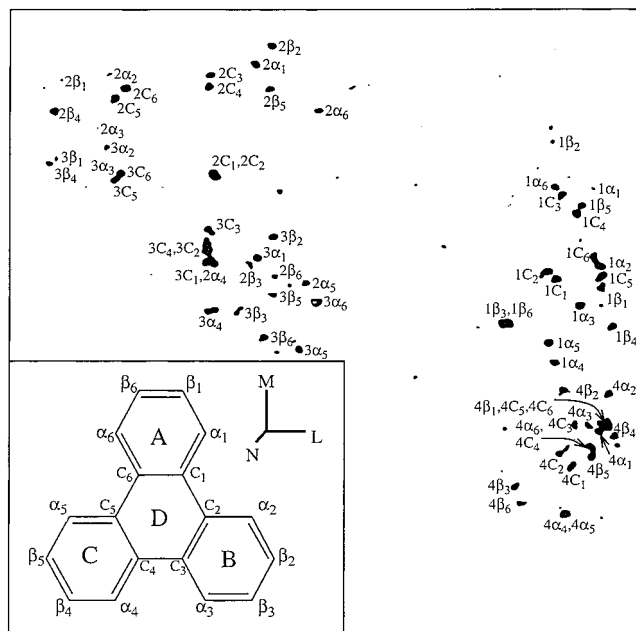


**Figure 1.** The 2D CS-CS spectra of triphenylene for the spherical shaped sample. The horizontal and vertical axes of the spectra are, respectively, the *xy* diagonal and *x* cardinal axes of the sample frame.<sup>7</sup> The lower left insert gives the molecular scheme of the triphenylene molecule with carbon position indices along with the axes of the molecular frame. Labels in the spectrum designate the 18 carbon atoms with numerals for each of the four congruent molecules, letters, in the unit cell. While some of the noise peaks are comparable to the lowest intensity signal peaks, they do not correlate with peaks in the other 2D spectra.

properly the congruent shifts with a given tensor and to establish the symmetry relationships between the congruent peaks. The tensors then may be determined in the typical linear least-squares fashion.<sup>7</sup> Thus, theoretically calculated tensors provide an initial assignment that is iterated with the experimental data until a self-consistent set of tensors are obtained which are independent of the initial theoretical estimates. Hence, the ultimate set of self-consistent tensors is no longer dependent upon any limitations in the initial theoretical calculations only in our ability to properly identify or assign the resonance peaks to designated molecules in the unit cell.

The single-crystal NMR spectrum of triphenylene reflects four molecules per unit cell and exhibits 72 magnetically nonequivalent carbon resonances that correspond to 18 chemically distinct <sup>13</sup>C nuclei. This 4-fold redundancy and the spatially well-characterized symmetry of the *D*<sub>2</sub> symmetry element, describing this unit cell, provides high confidence when a final set of self-consistent tensors is ultimately found. Although these chemical shift tensors for triphenylene may be determined, in principle, with only three distinct crystal orientations contained in two 2D CS-CS spectra with a common orientation, a third 2D spectrum, again with a common orientation with one of the two previous spectra, introduces an additional unique crystal orientation that increases the statistical confidence of the data analysis. Finally, even though it was not required, a fourth CS-CS spectrum of triphenylene, corresponding to the eventually aborted study of the cylindrical sample, provided additional confirming evidence of consistency in our final assignment. A 2D CS-CS spectrum of triphenylene is shown in Figure 1, where 65 of the possible 72 spectral peaks may be accounted for with 57 readily observed peaks. Some degeneracy reduces the 65 peaks to 57. Polarization efficiencies and other problems combined to eliminate 7 peaks (i.e., the difference between 65

and 72) from the spectrum, but this information is redundant and not fatal to the analysis.

The theoretical shielding tensors were calculated by the CHF/GIAO method<sup>19,20</sup> utilizing the D95V basis set.<sup>21</sup> The molecular geometry of triphenylene required to construct the wave functions was obtained from a neutron diffraction study.<sup>13</sup> The calculated shielding tensors were converted into the experimental shift scale with use of the relationship  $\delta_{ij} = m\sigma_{ij} - K_{ij}b$ ; where  $m = -1.12$ ,  $b = 209.7$  ppm, and  $K_{ij}$  is the Kronecker delta. The slope and intercept parameters for this relationship were determined by least-squares fitting of the experimental shifts and calculated shielding tensors of acenaphthene<sup>2</sup> and perylene.<sup>1</sup>

The calculated tensors are used to simulate the 72 chemical shifts of triphenylene for various orientations of the unit cell. To simulate all of the 2D peaks in a given spectrum only one transformation between the sample frame and the crystal symmetry frame is needed because the relationship between pairs of directions in a specified sample frame is known from the geometry of the flipper probe.<sup>7</sup> A good initial approximation for the transformation between the sample and symmetry frames may be recognized visually when the set of theoretically predicted and experimental shifts come into near correspondence between two overlaid spectra. Conversely, the simulated and experimental spectra fail to exhibit similar patterns whenever the frame transformation is seriously out of register. This is especially obvious when as many as 72 peaks are considered as a false transformation eliminates any correspondence between the predicted and observed spectra. Since all three 2D spectra were simulated simultaneously the constraints are even more pronounced than for a single 2D spectrum. Thus, the proper frame transformation is usually recognized after only a few initial trial-and-error approximations have been judiciously selected and attempted. Experience with the process greatly increases the facility with which frame identification is achieved.

The preliminary set of chemical shift tensors, based on the theoretical peak designations, is then completed and attention is directed solely to the usual least-squares method for analyzing the experimental data. Peak assignments are permuted among nuclei, primarily congruent sets, to see if the experimental root mean of the sum of squared residuals, *R*, will change. This is followed by a refinement in the frame transformations required to correct for small calibration errors in the crystal orientations of the sampling mechanism. Even though the four 2D NMR spectra of triphenylene have 72 peaks, and therefore an inordinately large number of possible permutations in the initial peak assignments, several factors aid in the judicious selection of the most likely assignments. First, the spectral peaks for each of the four triphenylene molecules per unit cell tend to cluster in groups and exhibit consistent patterns for each independent molecule because of the similarity in their structural features (i.e., the planarity of each aromatic ring system). This clustering may be readily noted in Figure 1. Second, the 5 ppm accuracy in the predictability of the theoretical calculations is sufficiently restrictive that only those permutations with theoretical peaks falling within a 5 ppm radius of experimental peaks need to be considered seriously in the visual selection of optimal fits. Convergence of this process for triphenylene, therefore, proceeded in a reasonable time period. Once satisfactory peak assignments and identification of the congruent peak relationships have been obtained for the three 2D spectra taken on the

(19) Ditchfield, R. *Mol. Phys.* **1974**, *27*, 789.

(20) Wolinski, K.; Hinton, J. F.; Pulay, P. *J. Am. Chem. Soc.* **1990**, *112*, 8251.

(21) Dunning, T. H.; Hay, P. J. In *Methods of Electronic Structure Theory*; Plenum: New York, 1977.

**Table 1.** The Cartesian  $^{13}\text{C}$  Chemical Shift Tensors of Triphenylene in the Unit Cell Frame<sup>a</sup>

	$\delta_{xx}$	$\delta_{yy}$	$\delta_{zz}$	$\delta_{xy}$	$\delta_{yz}$	$\delta_{zx}$
$\beta_1$	101.3	148.8	129.7	38.3	92.8	-52.5
$\beta_2$	133.4	161.1	86.2	79.5	48.5	-45.5
$\beta_3$	146.4	106.8	128.5	39.1	45.5	-94.6
$\beta_4$	105.0	139.6	132.9	30.6	95.4	-49.7
$\beta_5$	152.8	139.1	89.8	82.6	53.2	-37.6
$\beta_6$	151.4	102.1	124.1	44.1	41.5	-94.5
$\alpha_1$	129.9	149.8	86.5	78.9	57.5	-38.7
$\alpha_2$	95.7	155.8	116.0	36.0	84.3	-46.3
$\alpha_3$	100.2	141.6	129.8	29.1	83.7	-63.4
$\alpha_4$	146.7	101.4	125.8	36.0	58.3	-85.2
$\alpha_5$	160.5	98.2	108.1	42.7	43.0	-82.0
$\alpha_6$	137.8	140.5	84.6	81.0	41.6	-51.9
$C_1$	148.5	125.7	115.0	49.5	59.4	-80.7
$C_2$	143.6	128.8	115.9	47.6	58.1	-82.3
$C_3$	137.2	150.2	102.9	70.0	60.8	-60.6
$C_4$	142.7	143.9	102.6	70.6	63.3	-58.9
$C_5$	128.3	143.9	118.8	44.2	83.7	-61.9
$C_6$	123.0	148.7	116.9	45.7	80.4	-64.0

<sup>a</sup> Values of shifts given in ppm relative to TMS.

spherical sample, data from the single 2D spectrum from the cylindrical sample were also included in the tensor refinement process by using similar procedures.

When the above analysis was used to determine the 18 unique triphenylene tensors, the best fit resulted in a  $R$  value of 0.48 ppm for all 2D data sets. This error is well within the limits noted in previously measured PAH tensor studies.<sup>1,2</sup> The determined tensors are given in the Cartesian representations of the unit cell frame and as principal values with the directional cosines of their principal axes in the molecular frame. These two tensor representations are found in Tables 1 and 2, respectively. The molecular frame, depicted in the insert of Figure 1, is defined by an axis,  $N$ , normal to the molecular plane and an axis,  $M$ , linking the center of rings A and D, as well as the mutually perpendicular axis,  $L$ . The transformation between the unit cell and molecular frames is obtained by taking  $N$  along the average orientation of all  $\delta_{33}$  tensor components followed by a rotation about  $N$  to place the axes  $M$  and  $L$  in the defined location. This rotation angle about  $N$  is found by minimizing the chemical shift distance<sup>22</sup> between the sets of chemically congruent tensors assuming  $C_{3v}$  symmetry. It is once again emphasized that the final set of tensors is determined solely from properly assigned experimental data that conform to the symmetry of the crystal even though the procedure was initiated with theoretical tensors. Thus, uncertainties in the theoretical tensor values fail to propagate into the measurements of the experimental tensors.

When either the SA-CS-CS or CS-CS methods are used, the above procedure to find a symmetry frame requires a good initial assignment of congruent spectral peaks and the identification of the symmetry relationships that relate the corresponding peaks. These constraints still leave the transformation from the symmetry frame to the unit cell frame to be determined. For crystals with  $D_2$  symmetry, only one of the six permutational symmetry frames will correspond to the correct unit cell frame. The residual of the experimental fit, described above, is invariant to all these possible symmetry permutations, and the designation of the correct symmetry frame as the unit cell frame may be achieved only by establishing a correspondence between one of the permuted experimental tensors and the theoretically calculated tensor.<sup>22</sup> The best symmetry frame is recognized

**Table 2.** The Principal Values and Directional Cosine  $^{13}\text{C}$  Chemical Shift Tensors of Triphenylene in the Molecular Frame<sup>a</sup>

		$\delta_{11}$	$\delta_{22}$	$\delta_{33}$	$\delta_{\text{ave}}$	CP/MAS
$\beta_1$		232.9	143.6	3.3	126.6	126.4
	$\cos \theta_L$	0.523	0.852	0.001		
	$\cos \theta_M$	0.852	-0.523	-0.020		
	$\cos \theta_N$	0.016	-0.011	0.9998		
$\beta_2$		228.4	142.7	9.5	126.9	126.9
	$\cos \theta_L$	0.997	0.064	0.042		
	$\cos \theta_M$	0.064	-0.998	0.009		
	$\cos \theta_N$	0.043	0.007	0.9991		
$\beta_3$		232.5	142.6	6.6	127.3	126.9
	$\cos \theta_L$	0.455	0.889	0.042		
	$\cos \theta_M$	-0.890	0.456	-0.012		
	$\cos \theta_N$	-0.030	-0.032	0.9990		
$\beta_4$		233.2	137.1	7.3	125.9	125.9
	$\cos \theta_L$	0.465	0.884	-0.052		
	$\cos \theta_M$	-0.885	-0.466	-0.003		
	$\cos \theta_N$	0.027	0.044	0.9987		
$\beta_5$		229.5	142.0	10.3	127.3	127.5
	$\cos \theta_L$	-0.998	-0.013	-0.058		
	$\cos \theta_M$	0.0136	-0.999	-0.012		
	$\cos \theta_N$	-0.058	-0.013	0.9983		
$\beta_6$		233.6	139.1	4.9	125.9	125.9
	$\cos \theta_L$	-0.529	0.848	0.027		
	$\cos \theta_M$	0.848	0.530	-0.017		
	$\cos \theta_N$	0.029	-0.014	0.999		
$\alpha_1$		222.3	139.5	4.5	122.1	121.7
	$\cos \theta_L$	0.990	0.144	-0.005		
	$\cos \theta_M$	0.144	-0.990	-0.008		
	$\cos \theta_N$	0.006	-0.007	0.999		
$\alpha_2$		222.5	135.5	9.4	122.5	122.3
	$\cos \theta_L$	0.601	0.799	0.035		
	$\cos \theta_M$	0.799	-0.601	0.004		
	$\cos \theta_N$	-0.024	-0.026	0.999		
$\alpha_3$		224.5	142.4	4.8	123.9	123.8
	$\cos \theta_L$	-0.3608	0.929	0.046		
	$\cos \theta_M$	-0.9300	-0.368	-0.015		
	$\cos \theta_N$	0.003	-0.048	0.998		
$\alpha_4$		223.5	146.9	3.6	124.7	124.5
	$\cos \theta_L$	0.361	-0.932	-0.036		
	$\cos \theta_M$	-0.933	-0.361	-0.011		
	$\cos \theta_N$	0.003	-0.037	0.999		
$\alpha_5$		221.1	137.5	8.2	122.3	122.3
	$\cos \theta_L$	-0.596	0.803	-0.032		
	$\cos \theta_M$	0.802	0.597	0.018		
	$\cos \theta_N$	-0.034	0.015	0.999		
$\alpha_6$		220.6	138.6	3.8	121.0	120.9
	$\cos \theta_L$	-0.993	0.119	0.025		
	$\cos \theta_M$	0.119	0.993	-0.015		
	$\cos \theta_N$	0.026	0.012	0.999		
$C_1$		214.1	173.7	1.3	129.7	129.5
	$\cos \theta_L$	0.513	-0.858	-0.008		
	$\cos \theta_M$	-0.858	-0.513	0.016		
	$\cos \theta_N$	0.010	0.015	0.999		
$C_2$		213.2	173.3	1.8	129.5	129.5
	$\cos \theta_L$	-0.465	-0.885	0.032		
	$\cos \theta_M$	0.886	-0.464	0.017		
	$\cos \theta_N$	0.0	0.036	0.999		
$C_3$		214.3	174.9	1.1	130.1	129.8
	$\cos \theta_L$	-0.999	-0.049	0.023		
	$\cos \theta_M$	0.049	0.999	-0.002		
	$\cos \theta_N$	0.022	0.003	0.999		
$C_4$		214.1	175.2	-3.3	129.7	129.5
	$\cos \theta_L$	0.999	0.009	-0.008		
	$\cos \theta_M$	-0.009	0.999	-0.001		
	$\cos \theta_N$	0.008	-0.001	0.999		
$C_5$		216.8	172.8	1.4	130.4	130.2
	$\cos \theta_L$	0.472	0.881	-0.023		
	$\cos \theta_M$	0.882	-0.472	0.022		
	$\cos \theta_N$	-0.009	0.031	0.999		
$C_6$		215.4	172.7	0.6	129.6	129.5
	$\cos \theta_L$	-0.507	0.862	0.012		
	$\cos \theta_M$	-0.862	-0.507	0.018		
	$\cos \theta_N$	0.021	0.001	0.999		

<sup>a</sup> Values of shifts given in ppm relative to TMS.

when the root-mean-square (rms) chemical shift distance between the experiment and calculated tensor is minimal. The best result on triphenylene exhibited a rms distance of 4.2 ppm for all 18 tensors, while the second best permutation of symmetry frames had a distance, 7.5 ppm, that was measurably higher. The other four possibilities resulted in rms uncertainties that were an order of magnitude larger. The relatively large difference between the best and second best permutational assignment justifies confidence in quantum chemical calculations to provide the tensor assignment upon which the SA-CS-CS method depends.

A further confirmation of the tensor assignments is obtained by comparing their trace with the isotropic chemical shifts of a CP/MAS experiment. From Table 2 it is observed that the average of the tensor's trace reproduces the CP/MAS isotropic shifts well within the line widths (i.e., 0.6 ppm) of these peaks at half height. The largest discrepancy between the single-crystal and CP/MAS isotropic shifts, 0.4 ppm, is found at the two positions  $\alpha_1$  and  $\beta_3$ .

The rms of the residuals in the fit, when adjusted for the number of degrees of freedom, provides an estimate of the experimental uncertainty in measuring the two orientational shifts of a 2D spectral peak. Since the SA-CS-CS method is affected by crystal orientational errors in the measuring device, it is important to know how these errors propagate into the principal values and the nominal orientations of the principal axes in the molecular frame. These errors, based on the a similar procedure<sup>1</sup> used for perylene, reveal an average uncertainty of 0.35 ppm in the principal values of this molecule. This overall uncertainty in the in-plane principal components,  $\delta_{11}$  and  $\delta_{22}$ , varies between 0.2 and 0.5 ppm, whereas the errors in the perpendicular component,  $\delta_{33}$ , consistently were about 0.3 ppm.

The corresponding uncertainty in the orientational measurements, expressed as directional cosines relative to the three molecular axes (i.e.,  $M$ ,  $L$ ,  $N$ ), depends on both the direction and degree of anisotropy of the tensor components. The errors in all of the directional cosines for the  $\delta_{33}$  component are relatively small and these uncertainties reflect the large anisotropy between  $\delta_{33}$  and the in-plane principal values for  $\delta_{11}$  and  $\delta_{22}$ . Typical uncertainties in the directional cosines for  $\delta_{11}$  and  $\delta_{22}$  are also usually as low as 0.001 for  $\cos \theta_N$  and also many in-plane values of  $\cos \theta_L$  and  $\cos \theta_M$ . An exception is encountered in the instance of condensed carbon tensors where the errors could range as high as 0.008 for  $\cos \theta_L$  and  $\cos \theta_M$  when larger uncertainties result from the relatively smaller in-plane shift anisotropy, i.e., about 40 ppm. Thus, the  $\cos \theta_N$  for  $\delta_{11}$ ,  $\delta_{22}$ , and  $\delta_{33}$  as well as  $\cos \theta_L$  and  $\cos \theta_M$  for  $\delta_{33}$  were determined to be better than 0.001. These uncertainties are slightly larger than those found in the perylene study, likely because the larger perylene data set used six 2D spectra.

The SA-CS-CS method uses calculated shielding parameters for two purposes. First, these tensor parameters provide the initial step in the iterative process necessary for experimentally identifying sets of congruent peaks in the 2D spectra. Second, the theoretical shielding values eventually are used to designate a given molecule with a specific position identified with the asymmetric molecule in the unit cell. While the latter process leaves the asymmetric molecular assignment subject to the uncertainties in the calculations, the first application only initiates an iterative procedure that eventually becomes free of limitations in the theoretical calculations. For this identification to be correct, the iterative procedure must converge to a satisfactory set of congruent peaks, as was done herein with triphenylene data.

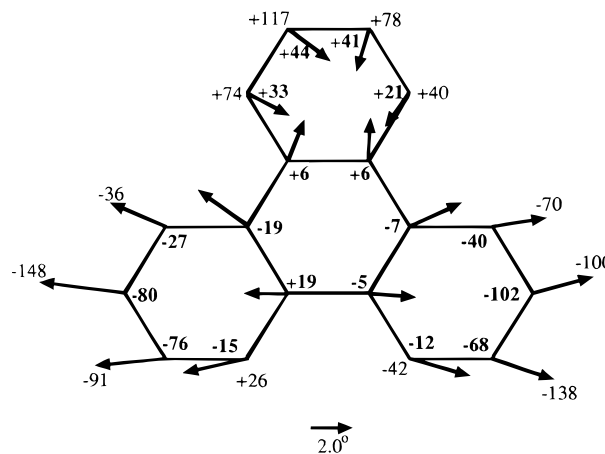


**Figure 2.** Diagram of the tilting of the  $\delta_{33}$  principal component. The vectors in the figure represent the direction,  $\tan^{-1}(\delta_{33} \cos \theta_L / \delta_{33} \cos \theta_M)$ ; the individual  $\delta_{33}$  tilt from the average  $\delta_{33}$  and the magnitude of the vectors,  $\cos^{-1}(\delta_{33} \cos \theta_N)$ , correspond to the angle between the individual  $\delta_{33}$  and the average  $\delta_{33}$ . The positions of both the hydrogen and carbon nuclei reported in the neutron study with respect to the best fit carbon plane are also shown here reported in 0.001 Å. The out-of-plane hydrogen positions are outside the rings, whereas the carbon positions, bold, are inside the rings.

### Discussion

The measured <sup>13</sup>C chemical shift tensors in triphenylene reveal both significant intermolecular and intramolecular crystalline effects for the three different types of carbon positions, i.e.,  $\alpha$ ,  $\beta$ , and C. The variations in shifts averaged about 5 ppm for corresponding principal components in the three chemical types of carbon atoms. The  $\alpha_4$  and  $\alpha_2$  positions varied the most, 11.4 ppm, for  $\delta_{22}$ . The orientational differences of the individual principal axis frame, PAF, are also experimentally significant as may be seen in Figure 2. The most important differences in the PAF orientations are due to planar deformations, which are believed to relieve the intramolecular strain of the bay hydrogen positions. These are reflected in the systematic tilt away from the normal to the aromatic ring, direction  $N$ , by the  $\delta_{33}$  orientational vectors shown in Figure 2. The exhibited vectors portray the buckling of the molecule with ring A bending toward the  $+N$  direction while rings B and C bend in a  $-N$  direction. The tilt in Figure 2 of the  $\delta_{33}$  principal axis at C<sub>1</sub> and C<sub>6</sub> into ring A was an unexpected feature. The tilt for the condensed carbons as well as the overall tilt was unexpected, but these orientations are consistent with the calculated tensors with diffraction structures that determine the deformation of the carbon backbone.

The distance<sup>22</sup> between two full chemical shift tensors is a single number that enables a direct comparison of both a tensor's principal values and their orientations. To calculate this distance between two tensors requires that they be placed in a common local reference frame that manifests the symmetry properties of the unit cell. By using the symmetry transformations of an idealized  $D_{3h}$  triphenylene molecule the tensors from each chemical group (i.e.,  $\alpha$ ,  $\beta$ , or C) may be compared in their corresponding local symmetry frames. The largest distance within a group of carbons is observed for the  $\beta$  tensors, i.e., 10.4 ppm, between positions  $\beta_5$  and  $\beta_4$ . Since only 2.9 ppm of the distance between the shift tensors at these two respective carbons may be attributed to the principal values, the relatively large distance of 10.4 ppm reflects a diversity in the orientations of the PAF. These results suggest considerable out-of-plane deformations of rings A and C with respect to the center ring. The two most similar tensors are found in the condensed carbons

**Table 3.** Molecular Symmetry Deviations in Triphenylene Determined by the Chemical Shift Distance

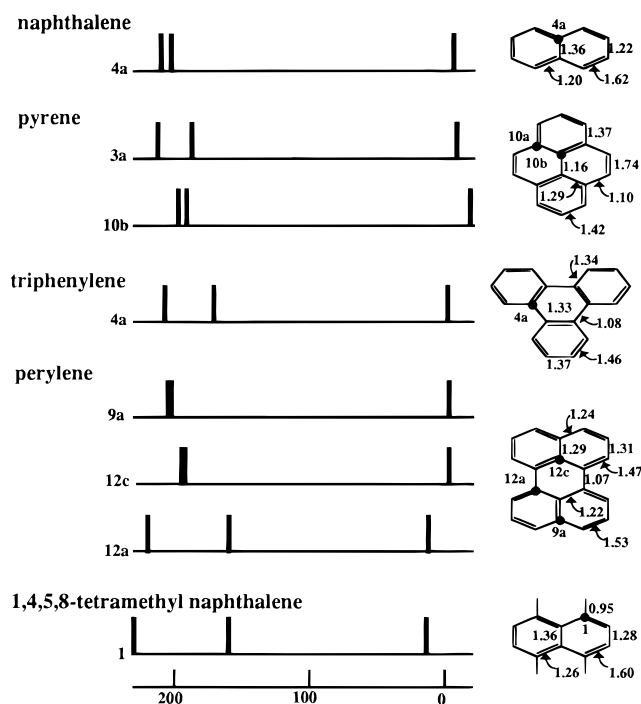
imposed symmetry	rms chemical shift distance <sup>a</sup>
$D_{3h}$	3.74
$C_{3v}$	3.30
$\sigma_{NM}$	1.21
$C_i$	0.48

<sup>a</sup> Values of root-mean-square (rms) shifts given in ppm.

of the center ring with a distance between positions  $C_1$  and  $C_4$  of only 1.51 ppm. An overall chemical shift distance between the six tensors of the three chemical groups in the molecule offers a criteria to test the breaks in these solid-phase molecular symmetries. Here, a rms distance was determined for the following assumed molecular symmetries:  $D_{3h}$ ,  $C_{3v}$ ,  $\sigma_{nm}$ , and  $C_i$  (see Table 3). The large discrepancies for the  $D_{3h}$  and  $C_{3v}$  symmetries indicate a failure to allow for planar deformations that destroy the  $C_3$  rotational symmetry. Yet, the planar distortion does not violate a vertical reflection plane and a good distance fit is observed for a  $\sigma_{nm}$  symmetry. The value for  $C_i$  symmetry is an estimate based on the variation of the tensor components as a function of spectral peak positions and hence has the same  $R$  value.

The benefits of determining the full chemical shift tensor may be appreciated in part from an analysis of the variations in the isotropic shift obtained in the CP/MAS experiment. The trace of the tensors or corresponding isotropic shifts reflect structural differences, but they fail to provide the geometric details or insight into the specific molecular structural deformations giving rise to these differences. For example, the largest tensor difference between two  $\alpha$ -carbons is found between positions  $\alpha_3$  and  $\alpha_4$ . Interestingly, this overall difference is concentrated primarily in only the  $\delta_{22}$  values. In comparison to the remaining  $\alpha$ -carbon tensors, the  $\alpha_3$  and  $\alpha_4$  tensors have large paramagnetic shifts in  $\delta_{22}$  of 142.4 and 146.9 ppm, which explains a difference in the isotropic paramagnetic shifts relative to the other  $\alpha$ -carbon tensors. This change in  $\delta_{22}$  may indicate a difference in the intramolecular strain of the bay hydrogen positions in the B-C region relative to the strain in the other bay regions. Bay-hydrogen strain also perturbs the  $\delta_{33}$  component. In comparison to other PAH protonated  $\alpha$ -carbons,<sup>1,2,15,23,24</sup>  $\delta_{33}$  is shifted diamagnetically by a relatively large value, 10–15 ppm, for  $\alpha$ -carbons.

The in-plane tensor components,  $\delta_{11}$  and  $\delta_{22}$ , are especially sensitive to variations in the local  $\pi$ -electron density. For aromatic  $sp^2$  carbons, the anisotropy between  $\delta_{11}$  and  $\delta_{22}$  reflects the noncylindrical distribution of  $\sigma$ -electrons in the molecular plane about the nucleus. Thus, the extent of electron delocalization and breaks in symmetry are sensitive to the in-plane anisotropy, allowing the aromaticity and  $\pi$ -electron delocalization of  $sp^2$  carbons to be differentiated and quantified. These data also correlate with C-C bond lengths and the related  $\pi$ -bond orders. Such correlations are depicted in Figure 3 for bond orders and the chemical shift anisotropy which may be as large as 40 ppm between the in-plane components,  $\delta_{11}$  and  $\delta_{22}$ , for the condensed carbons in triphenylene. These relationships relate to the electronic structure predicted by a simple Kekule model wherein the  $\pi$ -electron density in the C-C bonds linking the condensed carbons is suppressed. The in-plane anisotropy of condensed carbons in triphenylene is slightly smaller than

**Figure 3.** The principal values of condensed carbon in polycyclic aromatic hydrocarbons. Standard IUPAC nomenclature is used to label all carbon positions reported in this figure. At this scale, the trends and approximate values may be observed. The bond orders given in this figure were taken from Facelli and Grant.<sup>27</sup>**Table 4.** The Correlation of Theoretical Tensors to Experimental<sup>a</sup>

structure	slope	intercept shieldings	rms shift distance
X-ray	-1.10	207.8	7.38
X-ray optimized <sup>b</sup>	-1.12	210.4	4.23
neutron	-1.11	209.6	4.27
neutron optimized <sup>b</sup>	-1.11	210.0	4.07

<sup>a</sup> Values of intercept shieldings and root-mean-square (rms) shifts given in ppm. Intercept values are referenced to the bare nucleus. <sup>b</sup> Only the proton positions have been optimized.

that observed for the corresponding carbons in perylene at 12a and in tetramethylnaphthalene, indicating a modest increase in the  $\pi$ -electron character for the center ring. Nevertheless, the anisotropy still remains too large for these atoms to be characterized as normal bridgehead carbons in highly condensed PAH molecules, e.g., position 9a and 12c of perylene.

To compare variations in the molecular structure reported in diffraction studies with chemical shift tensor data, comparisons of the experimental tensors to theoretical tensors may be undertaken. All theoretical tensors depend acutely upon the molecular structure, and molecular quantum mechanics provides the connection between the two experimental quantities. Theoretical calculations were based on the GIAO method<sup>20</sup> with the D95V basis set.<sup>21</sup> Hydrogen positions were optimized with the GAUSSIAN 92 program<sup>25</sup> by using both neutron diffraction and X-ray structures.<sup>13,14</sup> These comparative results are reported in Table 4. The correlation slope and intercept was observed to be the same as noted in the previous study on perylene. Again no significant changes in these values were found for the different geometries. Without quantum-mechanical structure

(25) Frisch, M. J.; Trucks, G. W.; Head-Gordon, M.; Gill, P. M. W.; Wong, J. B.; Foresman, J. W.; Johnson, B. G.; Schlegel, H. B.; Rob, M. A.; Replogle, E. S.; Gomperts, J. L.; Andrees, J. L.; Raghavachari, K.; Binkley, J. S.; Gonzales, C.; Martin, R. L.; Fox, D. J.; Defrees, D. J.; Baker, J.; Stewart, J. J. P.; Pople, J. A. *GAUSSIAN 92*; Gaussain, Inc.: Pittsburgh.

(23) Carter, C. M.; Facelli, J. C.; Alderman, D. W.; Grant, D. M. *J. Am. Chem. Soc.* **1987**, *109*, 2639.

(24) Sherwood, M. H.; Facelli, J. C.; Alderman, D. W.; Grant, D. M. *J. Am. Chem. Soc.* **1991**, *113*, 750.

optimizations, the fit between the experimental tensors and the tensors calculated from the neutron diffraction geometry exhibit a rms distance of 4.27 ppm, which is currently the best observed for a PAH molecule. Another noted feature in Table 4 is the improvement in rms distance for the X-ray geometry after optimizing the hydrogen positions. This conclusion is consistent with the accepted assertion that neutron diffraction studies better determine the positions of hydrogen nuclei.<sup>26</sup> Further, the decrease from 7.38 ppm to 4.23 ppm, with optimization, suggests that the X-ray carbon geometry is of comparable quality with the neutron diffraction geometry. For the condensed carbon positions, the X-ray geometries do better than neutron structures with a rms fit of 2.97 versus 4.17 ppm, respectively. Conversely, the neutron structure gives better fits for the  $\alpha$ -carbon positions with a rms of 3.44 ppm compared to the 4.50 ppm for the X-ray geometry. Both geometries are similar at the  $\beta$  positions with rms fits of 4.74 and 4.48 ppm for X-ray and neutron structures, respectively.

### Conclusion

The improved resolution and inherent spatial correlation of 2D CS-CS over the traditional 1D rotational patterns are clearly demonstrated as advantages in the spectrum of triphenylene. By exploiting the crystalline symmetry of triphenylene, SA-CS-CS was used to determine all 72 magnetically different carbon nuclei in the unit cell arising from the 18 unique <sup>13</sup>C chemical shift tensors. By using only three, instead of six, 2D CS-CS spectra, the tensors were determined in 50% of the time used for the traditional CS-CS method with only modest loss in precision. Further, the successful incorporation of the second cylindrical sample's spectrum demonstrates the ability of SA-CS-CS to incorporate data from several single-crystal samples

(26) Jeffrey, G. A. Accurate Crystal Structure Analysis by Neutron Diffraction. In *Accurate Molecular Structures, Their Determination and Importance*; Domenicano, A., Hargittai, I., Eds.; Oxford University Press: New York, 1992; p 270.

(27) Facelli, J. C.; Grant, D. M. *Theor. Chim. Acta* **1987**, *71*, 277.

thereby verifying the flexibility of the method as shift tensors may be determined with three 2D CS-CS spectra without common crystal orientations. The use of the SA-CS-CS method relied on theoretical calculations of the shifts to make reliable initial peak assignments, hence the use of *ab initio* methods as a valuable spectroscopic tool.

The 18 unique <sup>13</sup>C chemical shift tensors of triphenylene describe the three sets (i.e.,  $\alpha$ ,  $\beta$ , and C) of six chemically similar carbon nuclei. These data on otherwise chemically similar positions reveal significant crystalline distortions that result in tensor diversity even for chemically similar carbons that differ by as much as 10.4 ppm. The most interesting crystalline distortions involve the break from planar symmetry, which is dramatically reflected in the  $\delta_{33}$  orientations. The tensors also suggest that a single effective vertical mirror plane exists in the molecule in contrast to the full crystalline space group of an isolated molecule. The intramolecular strain of the bay hydrogen positions is characterized by both the orientation and shift magnitudes of the  $\delta_{33}$  as well as the  $\delta_{22}$  values. The  $\pi$ -electron distribution is characterized by the in-plane anisotropy of the condensed carbon tensors, and for triphenylene,  $\pi$ -electrons delocalize primary in the peripheral rings. Finally, chemical shift comparisons of molecular structures interpreted with shielding calculations reveal X-ray data with optimized proton positions that compare favorably with neutron diffraction structures of triphenylene.

**Acknowledgment.** This work was supported by the Basic Energy Sciences at the Department of Energy through Grant No. DE FG02-94ER14452. Computer time was provided by an allocation from the University of Utah Center for High Performance Computing. We thank M. Solum for acquiring the CP/MAS data and further acknowledge D. W. Alderman for many helpful discussions on the subject.

JA972468G